FULLY AUTOMATED SPACE MAPPING OPTIMIZATION OF 3D STRUCTURES

J.W. Bandler, R.M. Biernacki and S.H. Chen

OSA-95-MT-28-R

November 30, 1995

FULLY AUTOMATED SPACE MAPPING OPTIMIZATION OF 3D STRUCTURES

J.W. Bandler, R.M. Biernacki and S.H. Chen

Optimization Systems Associates Inc.
P.O. Box 8083, Dundas, Ontario, Canada L9H 5E7

Tel 905 628 8228
Fax 905 628 8225
Email j.bandler@ieee.org

Abstract

We present new results of fully automating the aggressive Space Mapping (SM) strategy for electromagnetic (EM) optimization. The generic SM update loop and the model-specific parameter extraction loop are automated using a two-level Datapipe architecture. We apply the automated SM strategy to the optimization of waveguide transformers. We introduce a multi-point parameter extraction procedure for sharpening the solution uniqueness and improving the SM convergence. We present, for the first time, automated EM optimization utilizing the commercial 3D structure simulator HFSS.

This work was supported in part by Optimization Systems Associates Inc. and in part by the Natural Sciences and Engineering Research Council of Canada under Grants OGP0007239, OGP0042444 and STR0167080.

* The authors are also with the Simulation Optimization Systems Research Laboratory and Department of Electrical and Computer Engineering, McMaster University, Hamilton, Ontario, Canada L8S 4L7.

Manuscript submitted December 1, 1995.

SUMMARY

Introduction

The Space Mapping (SM) concept combines the computational expediency of empirical engineering models and the acclaimed accuracy of electromagnetic (EM) simulators [1-3]. In our original work, the initial mapping is established by aligning the two models at a number of base points. Our recent aggressive SM strategy drastically reduces the upfront effort by targeting every EM simulation at optimizing the design and progressively refining the mapping using the Broyden update [3, 4].

To implement the SM strategy requires two nested loops: the iterative process of updating the mapping and targeting the next EM simulation; and the parameter extraction process of aligning the empirical and EM model responses. The difficulty of manually carrying out these steps might discourage some engineers from exploiting the benefits of the SM concept.

We present new results of fully automating the aggressive SM strategy, using a two-level Datapipe architecture [5]. The outer level automates a generic aggressive SM loop including the Broyden update. The inner level implements parameter extraction for specific models, such as the Empipe™ interface to the EM simulator from Sonnet Software [5, 6].

We demonstrate the automated SM strategy on the optimization of both planar structures (a high-temperature superconducting filter) and 3D structures (waveguide transformers). We present, for the first time, automated SM optimization utilizing the commercial high-frequency structure simulator HFSS [7].

Parameter extraction is a crucial step in SM optimization. We investigate the impact of parameter extraction uniqueness on the convergence of the aggressive SM strategy. We introduce a multi-point parameter extraction approach to sharpening the solution uniqueness and improving the SM convergence.

The Space Mapping Concept

We consider models in two distinct spaces: the optimization space, denoted by X_{OS}, and the EM space, denoted by X_{EM}. We assume that the X_{OS} model is much faster to evaluate but less accurate than the X_{EM} model. The X_{OS} model can be an empirical model or a coarse-resolution EM model.

We wish to find a mapping P between the model parameters in these spaces:

$$x_{OS} = P(x_{EM}) \tag{1}$$

such that

$$R_{OS}(P(x_{EM})) \approx R_{EM}(x_{EM}) \tag{2}$$

where $R_{OS}(x_{OS})$ and $R_{EM}(x_{EM})$ denote the model responses in the respective spaces.

The purpose of SM is to avoid direct optimization in the computationally expensive X_{EM} space. We perform optimization in X_{OS} to obtain the optimal design x_{OS}^* and then use SM to find the mapped solution in X_{EM}.

$$\bar{x}_{EM} = P^{-1}(x_{OS}^*) \tag{3}$$

assuming that P is invertible.

In our original work [1, 2], the initial mapping is established by performing upfront EM analyses at a number of base points. Our recent aggressive SM strategy minimizes the upfront effort by targeting every EM simulation at optimizing the design and progressively refining the mapping [3].

Assuming that x_{OS} and x_{EM} have the same dimension, we start with

$$x_{EM}^1 = x_{OS}^* \tag{4}$$

At the ith step, if the EM analysis at x_{EM}^i produces the desired responses, then we have found a solution. Otherwise, we perform parameter extraction to find x_{OS}^i which minimizes

$$\| R_{OS}(x_{OS}^i) - R_{EM}(x_{EM}^i) \| \tag{5}$$

where $\|\cdot\|$ denotes a suitable norm, such as the ℓ_1 norm [8].

The next iterate is given by

$$x_{EM}^{i+1} = x_{EM}^{i} + h^i \tag{6}$$

The increment h^i is the solution to the linear system

$$B^i h^i = x_{OS}^{*} - x_{OS}^{i} \tag{7}$$

where B^i represents an approximate Jacobian matrix of the mapping P. We set B^1 to the identity matrix. In subsequent iterations we apply the Broyden update [3, 4]

$$B^{i+1} = B^i + \frac{x_{OS}^{i+1} - x_{OS}^{i} - B^i h^i}{(h^i)^T (h^i)} (h^i)^T \tag{8}$$

Automated SM Optimization

By inspecting the steps involved in the SM optimization, we recognize that the parameter extraction process of finding x_{OS}^{i} by minimizing (5) is explicitly dependent on the specific models involved. The other steps, as defined by (4), (6), (7) and (8), can be implemented within a generic layer of iterations.

Following this guideline, we fully automated the aggressive SM strategy using a two-level Datapipe architecture. The flow chart in Fig. 1 illustrates the two iterative loops involving two different sets of variables. The outer loop updates x_{EM} based on the latest mapping. The inner loop performs parameter extraction in which x_{OS} represents the variables and x_{EM}^{i} is held constant. The Datapipe techniques allow us to carry out the nested optimization loops in two separate processes while maintaining a functional link between their results (e.g., the next increment to x_{EM} is a function of the results of parameter extraction).

The inner loop must be set up according to the specific pair of models used. Within this loop, we can also utilize the Datapipe techniques to connect external model simulators to the optimization environment (e.g., our Empipe system is a specialized Datapipe interface to the EM simulator from Sonnet Software [5, 6]).

HTS Filter Design by SM Optimization

We have applied the aggressive SM strategy to the optimization of a high-temperature superconducting filter [2, 3]. The empirical microstrip coupled-line model (X_{OS} model) is not accurate for the high dielectric constant (23.425) of the lanthanum aluminate substrate. We use the ***em*** simulator [6] as the X_{EM} model (approximately 1 CPU hour on a Sun SPARCstation 10 is needed to simulate the filter at a single frequency with fine resolution).

Our automated SM optimization essentially reproduced the design reported in [3]. Six variables are optimized (the coupled-line section lengths L_1, L_2 and L_3 and the section spacings S_1, S_2 and S_3). Fig. 2 depicts the steps taken by x_{EM} projected onto minimax contours in the S_2-S_3 plane.

SM Optimization of Waveguide Transformers

We extend the automated SM optimization to waveguide structures, using first an empirical simulator and then the commercial 3D structure EM simulator HFSS.

The waveguide transformers under consideration are classical examples of microwave design optimization [9]. Fig. 3 depicts a typical two-section waveguide transformer.

First, we apply the SM strategy to two empirical models: an "ideal" model which neglects the junction discontinuity and a "nonideal" model which includes the junction discontinuity [9].

We optimized three designs, of two-, three- and seven-sections, respectively, using the automated SM strategy with successful results. The variables are the heights and lengths of the waveguide sections. Figs. 4 to 6 show the responses before and after SM optimization. The numbers of SM iterations required to reach the solutions are 7, 6 and 5, respectively.

We then embedded the commercial 3D structure EM simulator HFSS into the automated SM optimization loop. We developed a suitable interface based on Geometry Capture [10] in order to parameterize 3D structures, drive HFSS and capture the results in an automated manner. Four variables are involved, namely the heights and lengths of the two waveguide sections. The solution shown in Fig. 7 requires 10 SM iterations (hence 10 HFSS simulations).

Impact of Parameter Extraction Uniqueness

We use the two-section waveguide transformer example to investigate the impact of parameter extraction uniqueness on the convergence of the SM strategy. We observe symmetrical ℓ_1 contours with respect to the two section lengths L_1 and L_2, as illustrated in Fig. 8, with two local minima. Consequently the result of parameter extraction is not unique. The impact can be seen in the trace depicted in Fig. 9, where the SM steps oscillate around the solution due to the "fuzzy" results of parameter extraction.

We introduce a multi-point parameter extraction approach to sharpening the parameter extraction result. Instead of minimizing (5) at a single point, we find $\boldsymbol{x}_{OS}^{i}$ by minimizing

$$\| \boldsymbol{R}_{OS}(\boldsymbol{x}_{OS}^{i} + \Delta\boldsymbol{x}) - \boldsymbol{R}_{EM}(\boldsymbol{x}_{EM}^{i} + \Delta\boldsymbol{x}) \| \tag{9}$$

where $\Delta\boldsymbol{x}$ represents a small perturbation to $\boldsymbol{x}_{OS}^{i}$ and $\boldsymbol{x}_{EM}^{i}$. By simultaneously minimizing (9) with a selected set of $\Delta\boldsymbol{x}$, we hope to improve the uniqueness of parameter extraction. Conceptually, we are attempting to match not only the response, but also a first-order change in the response with respect to small perturbations in the parameter values. We have exploited a similar concept in multi-circuit modeling [11]. Fig. 10 depicts the ℓ_1 contours for multi-point parameter extraction of the two-section transformer, which indicates a unique solution. We used three points (i.e., three different $\Delta\boldsymbol{x}$) for parameter extraction. The corresponding SM trace is shown in Fig. 11, where the convergence of the SM strategy is dramatically improved. The price we pay for such an improvement is the increased number of EM simulations required.

Conclusions

We have presented new results of automating the aggressive SM optimization strategy. We believe that the automation will make the benefits of the SM approach more tangible in a practical sense. We have presented the first results of driving the commercial 3D full-wave simulator HFSS for the optimization of 3D structures. We have demonstrated the importance of unique parameter extraction in the SM process and introduced the multi-point approach to enhancing the prospect of a unique solution.

References

[1] J.W. Bandler, R.M. Biernacki, S.H. Chen, P.A. Grobelny and R.H. Hemmers, "Space mapping technique for electromagnetic optimization," *IEEE Trans. Microwave Theory Tech.*, vol. 42, 1994, pp. 2536-2544.

[2] J.W. Bandler, R.M. Biernacki, S.H. Chen, W.J. Getsinger, P.A. Grobelny, C. Moskowitz and S.H. Talisa, "Electromagnetic design of high-temperature superconducting microwave filters," *Int. J. Microwave and Millimeter-Wave CAE*, vol. 5, 1995, pp. 331-343.

[3] J.W. Bandler, R.M. Biernacki, S.H. Chen and R.H. Hemmers, "Electromagnetic optimization exploiting aggressive space mapping," *IEEE Trans. Microwave Theory Tech.*, vol. 43, December 1995.

[4] C.G. Broyden, "A class of methods for solving nonlinear simultaneous equations," *Math. of Comp.*, vol. 19, 1965, pp. 577-593.

[5] *OSA90/hope*™ and *Empipe*™, Optimization Systems Associates Inc., P.O. Box 8083, Dundas, Ontario, Canada L9H 5E7, 1995.

[6] ***em***™ and ***xgeom***™, Sonnet Software, Inc., 135 Old Cove Road, Suite 203, Liverpool, NY 13090-3774, 1995.

[7] *HFSS*, Hewlett-Packard Co., 1400 Fountaingrove Parkway, Santa Rosa, CA 95403, 1994.

[8] J. Hald and K. Madsen, "Combined LP and quasi-Newton methods for nonlinear ℓ_1 optimization," *SIAM J. Numerical Analysis*, vol. 22, 1985, pp. 68-80.

[9] J.W. Bandler, "Computer optimization of inhomogeneous waveguide transformers," *IEEE Trans. Microwave Theory Tech.*, vol. MTT-17, 1969, pp. 563-571.

[10] J.W. Bandler, R.M. Biernacki, Q. Cai, S.H. Chen and P.A. Grobelny, "Integrated harmonic balance and electromagnetic optimization with Geometry Capture," *IEEE MTT-S Int. Microwave Symp. Dig.* (Orlando, FL), 1995, pp. 793-796.

[11] J.W. Bandler and S.H. Chen, "Circuit optimization: the state of the art," *IEEE Trans. Microwave Theory Tech.*, vol. 36, 1988, pp. 424-443.

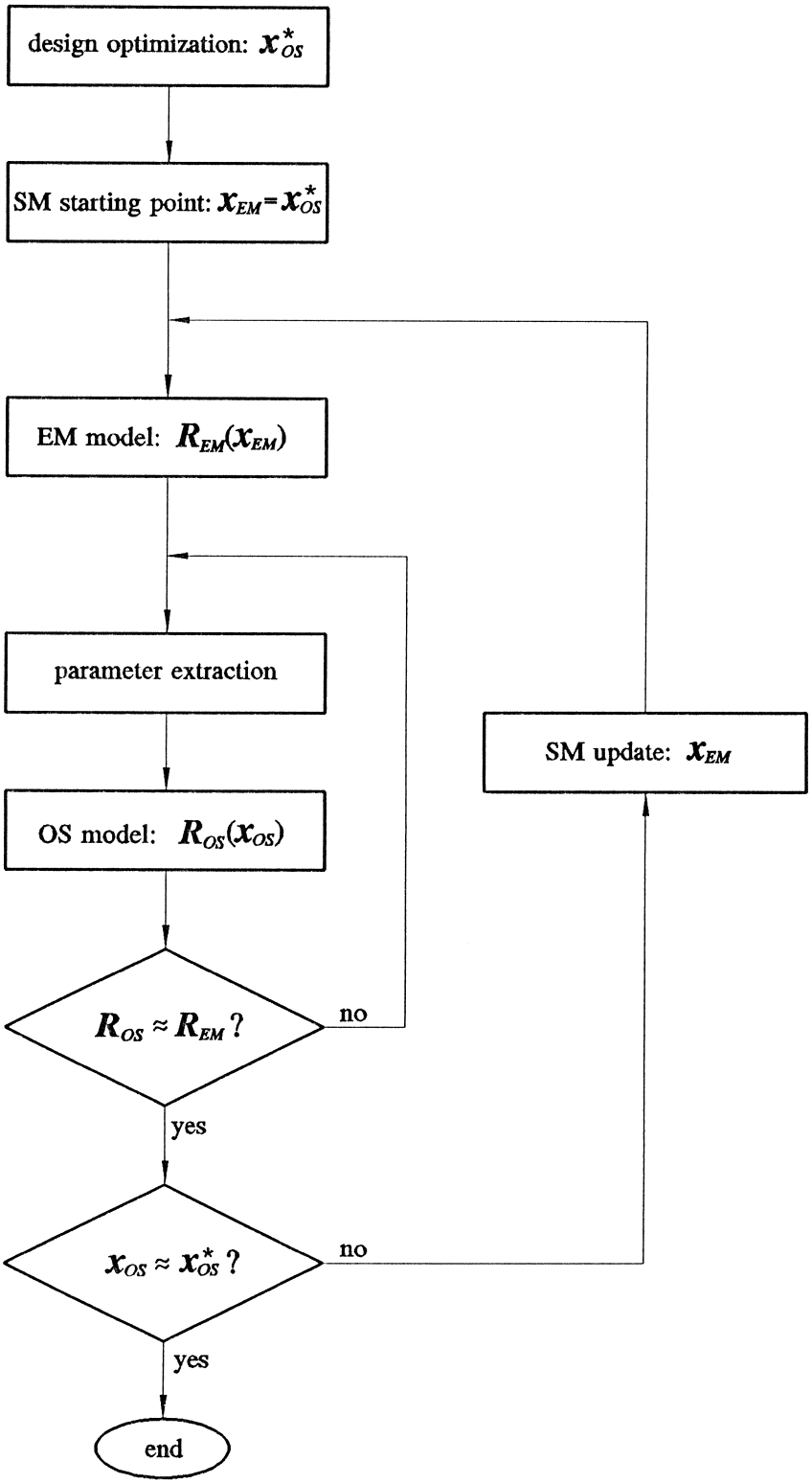

Fig. 1. Flow chart of the automated aggressive SM strategy.

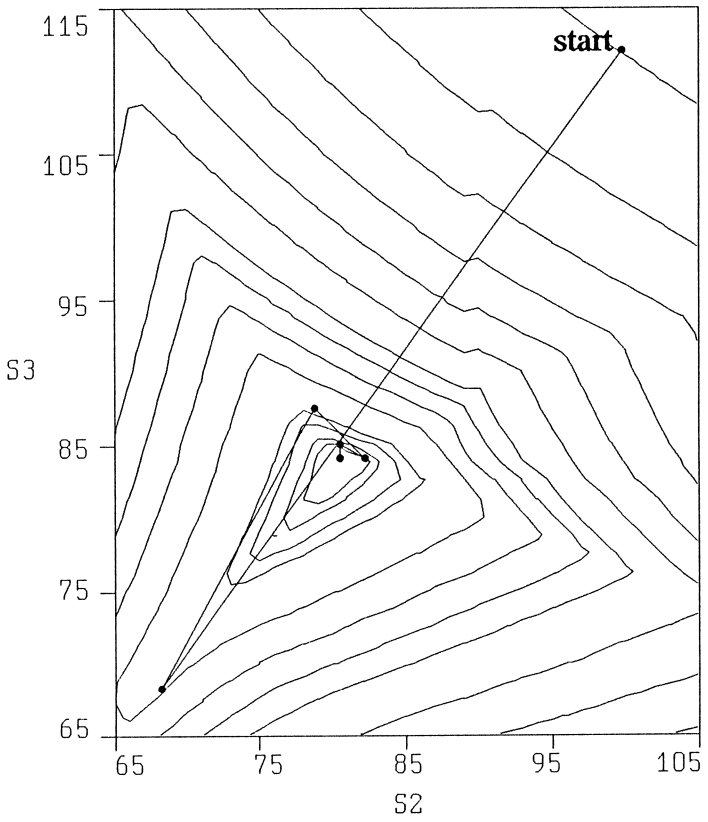

Fig. 2. Trace of the aggressive SM optimization steps of the HTS filter projected on the minimax contours of the S_2-S_3 plane.

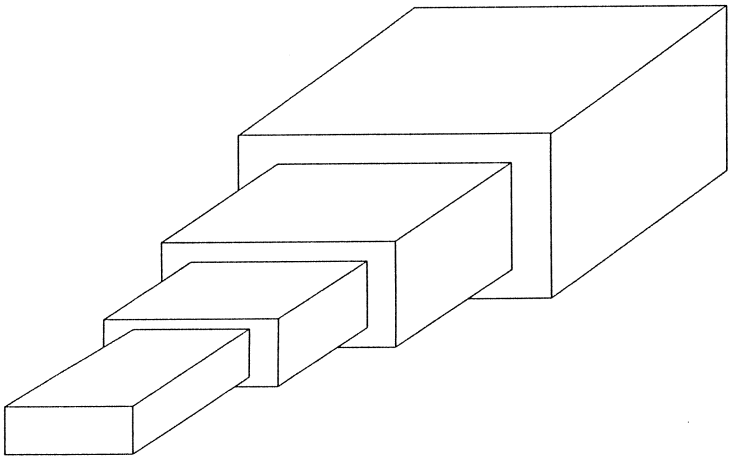

Fig. 3. A typical two-section waveguide transformer.

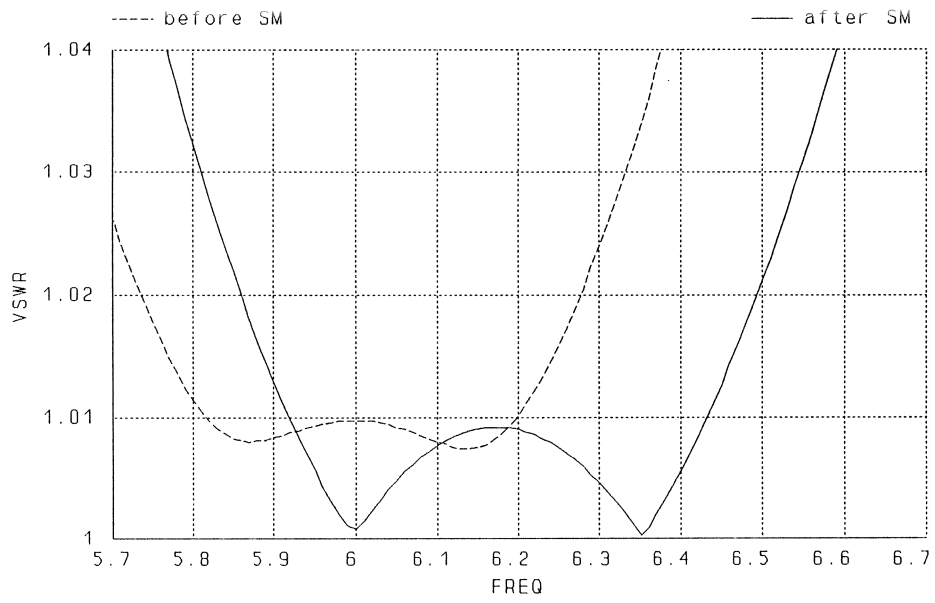

Fig. 4. VSWR response of the two-section waveguide transformer [9] simulated using the nonideal model before and after SM optimization. The response after 7 SM iterations is indistinguishable from the optimal ideal response. The frequency is in GHz.

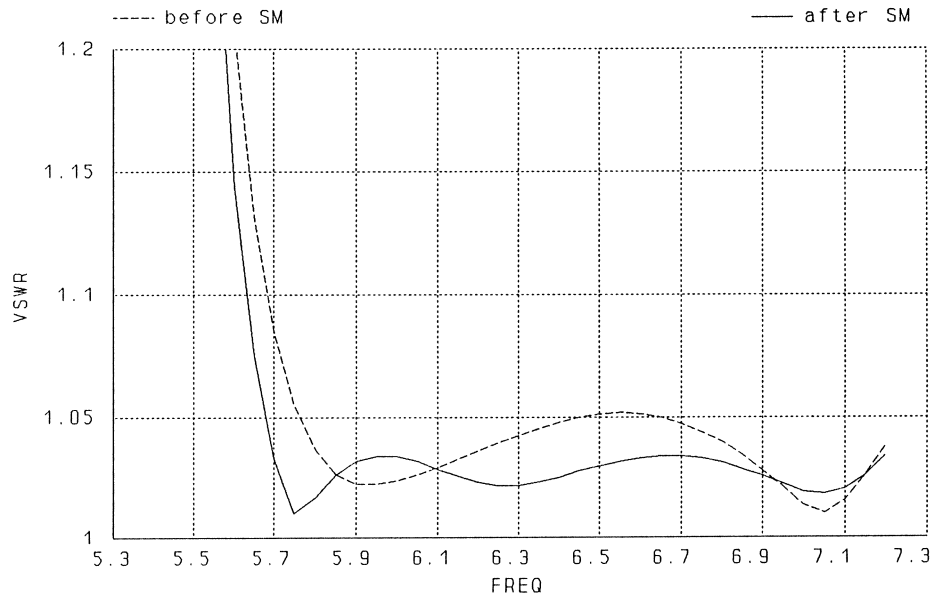

Fig. 5. VSWR response of the three-section waveguide transformer [9] simulated using the nonideal model before and after SM optimization. The response after 6 SM iterations is indistinguishable from the optimal ideal response. The frequency is in GHz.

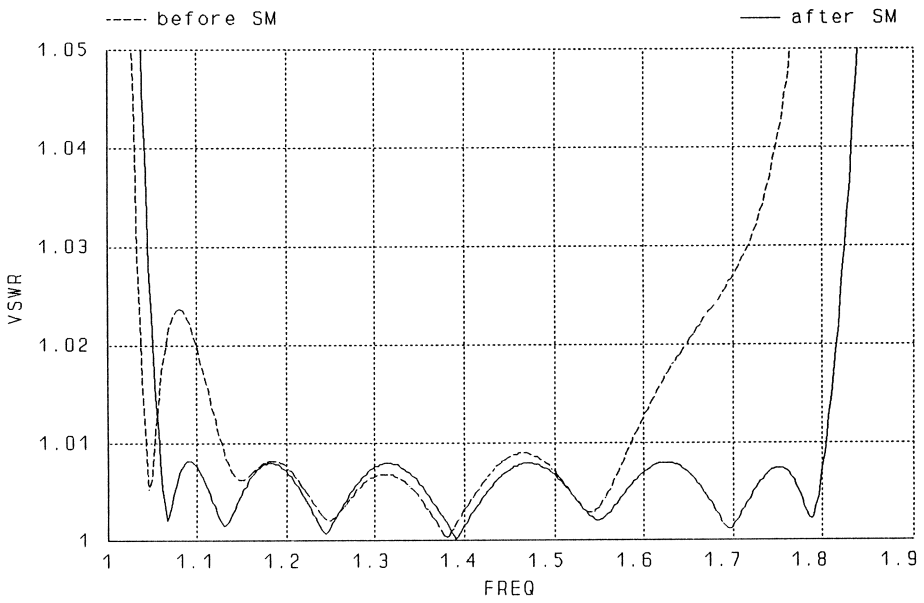

Fig. 6. VSWR response of the seven-section waveguide transformer [9] simulated using the nonideal model before and after SM optimization. The response after 5 SM iterations is indistinguishable from the optimal ideal response. The frequency is in GHz.

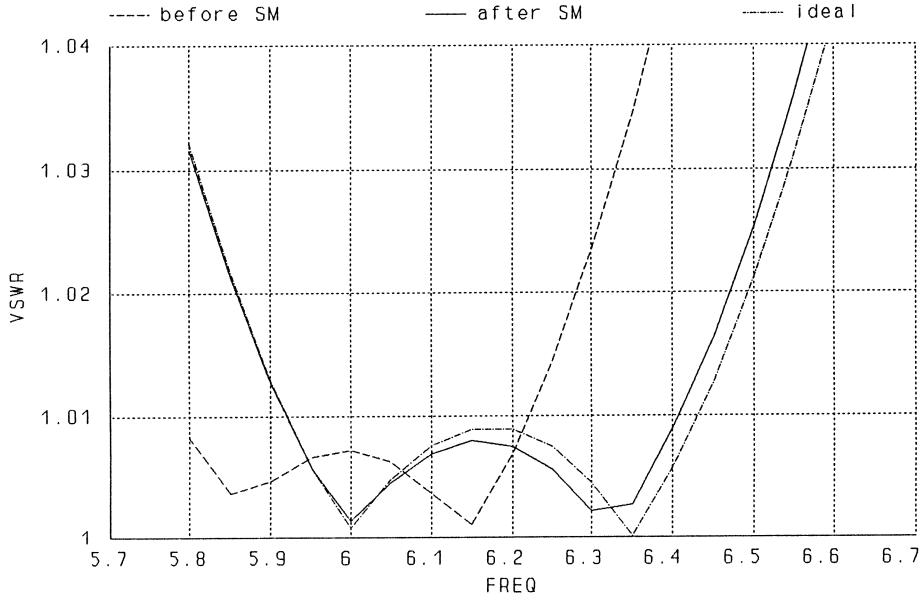

Fig. 7. VSWR response of the two-section waveguide transformer simulated by HFSS before and after 10 SM optimization iterations. Also shown is the optimal ideal response. The frequency is in GHz.

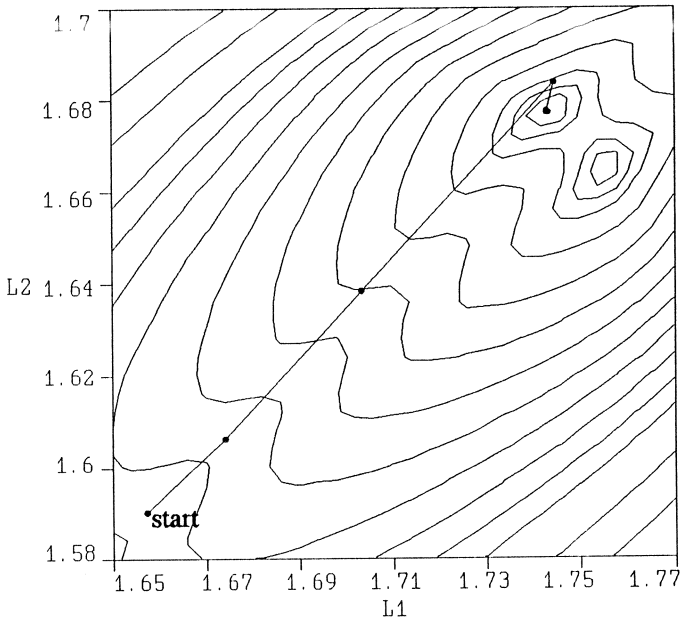

Fig. 8. The ℓ_1 contours of the parameter extraction problem for the two-section waveguide transformer. The symmetry between the variables L_1 and L_2 produces two local minima. Consequently the result of parameter extraction is not unique.

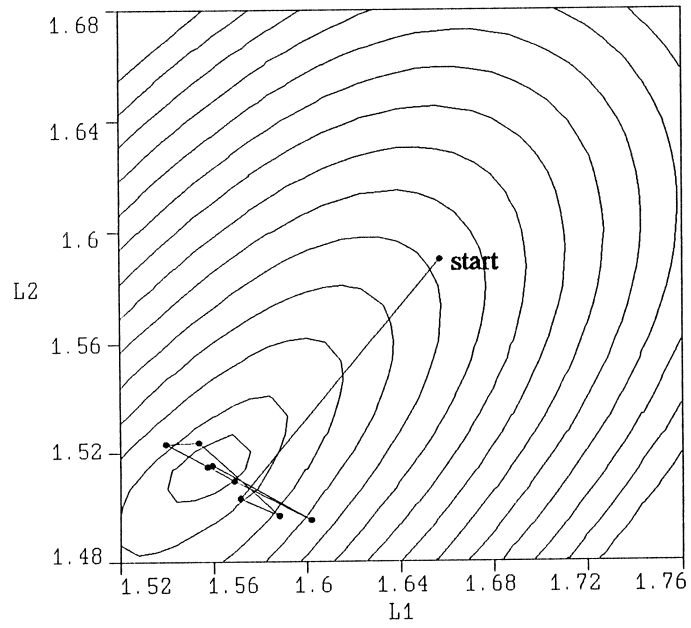

Fig. 9. Trace of the SM steps of the two-section waveguide transformer projected onto the minimax contours in the L_1-L_2 plane. The non-unique parameter extraction results lead to the SM steps oscillating around the solution.

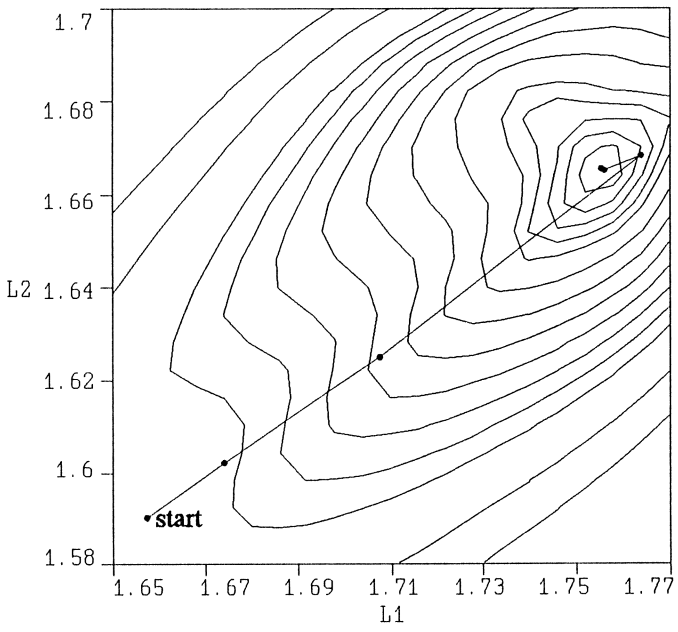

Fig. 10. The ℓ_1 contours of multi-point parameter extraction of the two-section waveguide transformer. The parameter extraction has a unique solution.

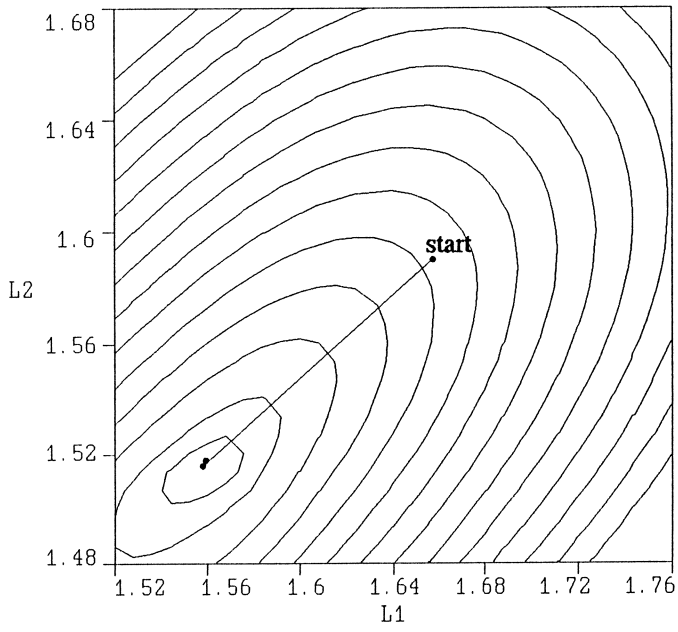

Fig. 11. Trace of the SM optimization with multi-point parameter extraction of the two-section transformer projected onto the minimax contours in the L_1-L_2 plane. The convergence is dramatically improved when compared with Fig. 9.